ITERATIVE LANDMARK PAIR PRUNING FOR LARGE-SCALE HISTOPATHOLOGY IMAGE REGISTRATION ENHANCEMENT

Runze Leng

Department of Mathematics and Statistics, Georgia State University, Atlanta, GA,30301

ABSTRACT

Three-dimensional (3D) digital pathology analysis is an emerging research topic in tissue-based cancer research. For 3D histology structure reconstruction, histopathology images of serial tissue sections need to be accurately aligned. To boost the histopathology image registration performance, we propose, in this paper, a registration enhancement method that iteratively improves landmark pair matching accuracy with multiple similarity metrics. Weak matched landmark pairs are iteratively trimmed based on spatial constraints. We apply this pruning method to a simulation and a real histopathology image dataset with the similarity measure determined by multiple methods. The landmark pair accuracy is increased on average by 42.6% in the simulation experiments. Furthermore, our enhancement method results in a registration improvement in the real histopathology image dataset by 35.23% (correlation), 17.56% (structural similarity), 6.30% (mutual information), and 48.78% (mean squared error), respectively. The qualitative and quantitative results from these experiments demonstrate the effectiveness of our method for registration improvement regardless of methods for similarity computation, suggesting the promise of our proposed method for large-scale pathology image registration.

Index Terms— 3D histology analysis, serial pathology image registration, landmark pair pruning

1. INTRODUCTION

Two-dimensional (2D) histopathology images analysis has been the mainstream research topic in tissue based cancer research [1, 2, 3, 4, 5]. Despite its great success, it is subject to significant histology information loss and bias. By contrast, the three-dimensional (3D) tissue volume analysis can address such limitations resulting from the 2D tissue slide sampling process [6, 7, 8, 9]. However, the formidable histopathology images of serial tissue slides becomes a major technical hurdle that prevents conversion of 2D serial tissue slides to 3D microscopy image volumes. As a whole slide histopathogy image can capture fine details of tissue phenotypic features, the premise for biological meaningful 3D histopathology image analysis is the accurate image registration. Prior efforts have been made to develop multiple methods designed to solve this problem, such as the region-based diffeomorphic registration method [10] and the patch-based discrete registration algorithm [11]. However, the giga-pixel scale of such histopathology images makes it impossible to apply them directly. Furthermore, histopathology tissues can be significantly deformed due to impacts of multiple forces during the image preparation process, such as bending, shearing, stretching, and tearing. Both the global and local tissue deformations make serial histopathology image registration a challenging task.

We have previously proposed a pioneering method that dynamically registers 3D subvolumes from serial gigapixel whole slide images using optimal spatial transformations estimated at low resolution representation [12]. By such a method, global and local tissue deformations can be largely compensated such that serial image regions are approximately aligned. However, such transformations mapped down from low resolution need to be further fine tuned with high resolution image content details. To support such fine-tuning process necessary for 3D histology analysis of small scale histology structures, we present, in this paper, a registration fine tuning method that iteratively assess and pruning matched landmark pairs by spatial constraints and similarity measures. Such post-processing method can effectively improve the serial histopathology image registration accuracy to potentially support the 3D pathology analysis at the cellular scale.

2. METHOD

The workflow for the proposed method has three steps: 1) generation of the initially matched landmarks by similarity metrics, 2) identification of the initial trusted landmark pairs by local spatial constraints, and 3) iterative outlier removal and trusted pair update.

We use a nuclei detection method to locate the

Some author footnote.

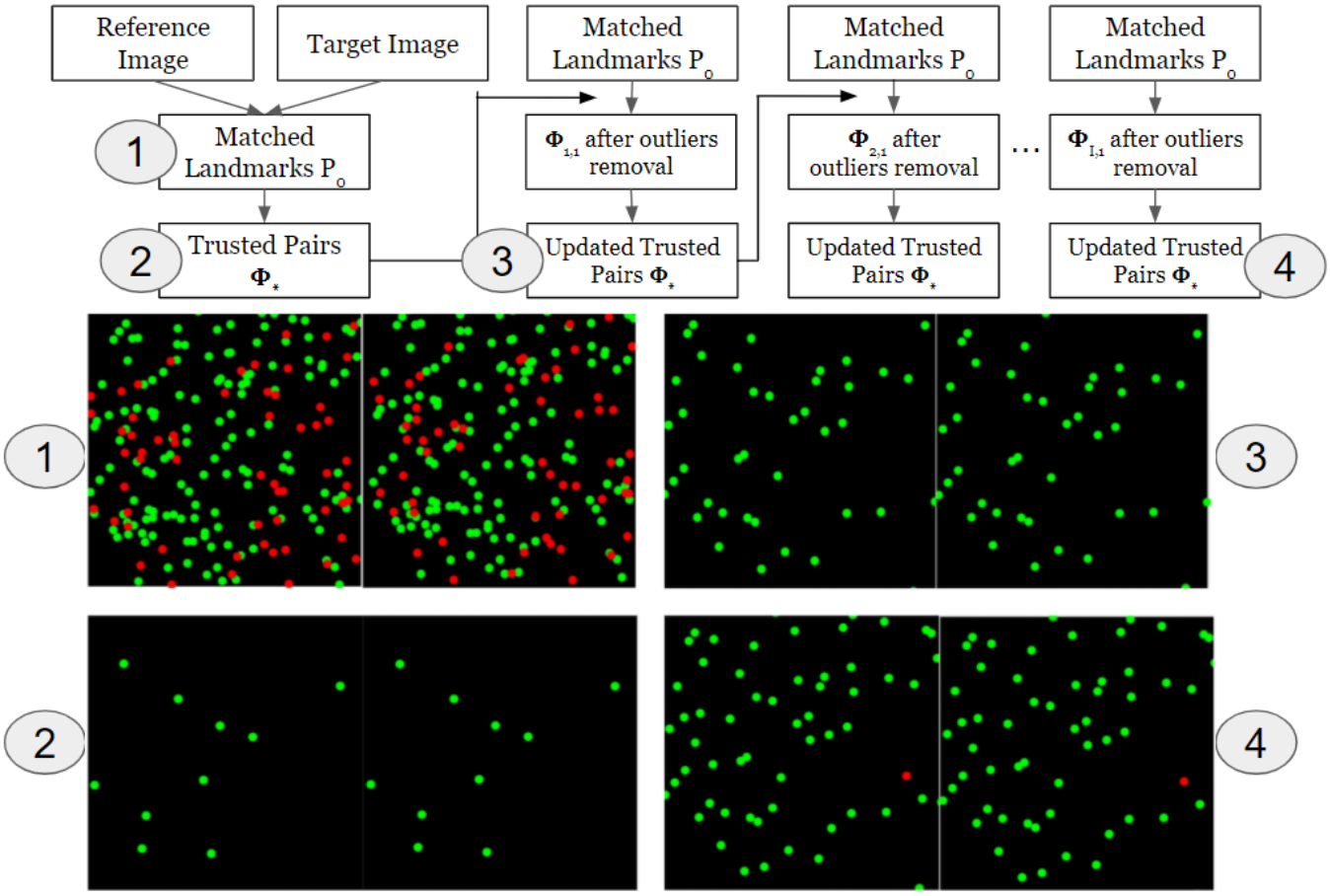

Fig. 1. Schema of proposed registration fine-tuning method by iterative landmark pair pruning and similarity assessment.

initial landmark candidates [13]. Normalized Cross-Correlation (NCC) are used to match the resulting landmarks. We denote a landmark pair as $p = \{\xi^r, \xi^t\} \in P_0$, where P_0 is the set of all retrieved landmark pairs and p represents two points (i.e. ξ^r, ξ^t) in each landmark pair. We denote $\xi^r = (X^r, Y^r)$ as a point in the reference image while $\xi^t = (X^t, Y^t)$ is a matched point in the target image. In the target image, the i-th nearest detected landmark to ξ^t is denoted as $\xi_i^t = (X_i^t, Y_i^t)$ where $i = 1, 2, ..., n$. The corresponding landmark from the reference image is denoted as $\xi_i^r = (X_i^r, Y_i^r)$. Note ξ_i^r may or may not be the i-th nearest landmark to ξ^r in the reference image. Furthermore, $p_i(p) = (\xi_i^r, \xi_i^t)$ denotes a landmark pair with ξ_i^t from the target image being the i-th nearest landmark to $\xi^t \in p$ where $i = 1, 2, ..., n$. We next compute the distance between ξ^t and ξ_i^t from the target image, and the distance between ξ^r and ξ_i^r from the reference image:

$$\delta_i^k = |X_i^k - X^k|, \gamma_i^k = |Y_i^k - Y^k|, i = 1, 2..., n,\ k = \{t, r\}$$

Next, we characterize the local neighboring patterns by the local distance ratios of the n nearest landmarks in the reference to those in the target image by x- and y-coordinate, respectively:

$$S^x(p_i) = \frac{\delta_i^r}{\delta_i^t}, S^y(p_i) = \frac{\gamma_i^r}{\gamma_i^t}, i = 1, 2..., n$$

In order to identify the trusted pairs, we define four important parameter, p, P, n, and r. We denote matched landmark pair candidate as p; P is a set that includes all possible landmark pair candidates; We define n, and r as the number of closest landmark pairs and the cutoff value for the local distance ratio. We iteratively apply the following function to remove outlines and construct a set of trusted pairs:

$$F(p, P, n, r) = \{q \,|\, q \in \mathcal{N}(p, n) \subset P, \frac{1}{r} < S^x(q), S^y(q) < r\}$$

where $\mathcal{N}(p, n)$ represents the n closest landmark pairs to p.

After we this step, we identify the trusted landmark pair set Φ^* by applying the function $\Phi_{k+1} =$

$F(\phi_k, \Phi_k, n_1, r)$ K_1 times, with $\phi_1 = p, \Phi_1 = P_0$ and $\Phi^* = \Phi_{K_1+1}$. In these iterations, a pair is considered as an outlier if any of its n_1 nearest pairs in Φ_k is more than r by local distance ratio.

After we have the trusted pairs, we use them to remove outliers one time, by applying the function $\Phi_{i,1} = F(p, \Phi^*, n_2, r)$, the more outliers removed in this step, we can use remained pair set after outliers removal to find more new trusted pairs Φ_{i,K_2+1} by applying the functions $\Phi_{i,k+1} = F(\phi_{i,k}, \Phi_{i,k}, n_3, r))$ $\frac{K_2}{2}$ times and $\Phi_{i,k+1} = F(\phi_{i,k}, \Phi_{i,k}, n_4, r))$ $\frac{K_2}{2}$ times. We will updated the trusted pairs by combine the trusted pairs that used in outliers removal step Φ^* and the new trusted pairs Φ_{i,K_2+1} together, which is $\Phi^* = \Phi^* \cup \Phi_{i,K_2+1}$. Then we test the updated trusted pairs by function $\Phi^* = F(\phi^*, \Phi^*, n_1, r)$ to make sure there is no outliers that falsely identified as trusted pairs.

The updated trusted pairs is more than and better(more even) distributed than the old trusted pairs. Therefore, we can use updated trusted pairs to remove more outliers in the next outliers removal step, and the remaining pair set with less outliers $\Phi_{i,1}$ will be able to give us more and better distributed new trusted pairs.

In total, we will do the removal step I times, under each time, it will be followed $\frac{K_2}{2}$ iterations of function $\Phi_{i,k+1} = F(\phi_{i,k}, \Phi_{i,k}, n_3, r))$ and another $\frac{K_2}{2}$ iterations of function $\Phi_{i,k+1} = F(\phi_{i,k}, \Phi_{i,k}, n_4, r))$ to find new trusted pairs. Then, combining the new trusted pairs with the old one to the updated trusted pairs and testing it. We will have I versions of updated trusted pairs in I times' removal steps. The I-th version of updated trusted pairs Φ^* will be the output of our pruning and selection algorithm. The final spatial transformation is derived by interpolation with these landmarks in Φ^*.

Algorithm 1 Identification of Trusted Landmark Pairs

Input: $\{R, T\}$: A reference and target image pair
Output: $\Phi_{*:}$ Final trusted landmark pairs

Extract landmark pairs $p \in P_0$
for $k \in (1, 2, ..., K_1)$ **do**
  $\phi_1 = p, \Phi_1 = P_0$
  $\Phi_{k+1} \leftarrow F(\phi_k, \Phi_k, n_1, r)$ ▷ $\phi_k \in \Phi_k$
$\Phi^* = \Phi_{K_1+1}$
for $i \in (1, 2, ..., I)$ **do**
  $\Phi_{i,1} \leftarrow F(p, \Phi^*, n_2, r)$ ▷ $\phi_{i,k} \in \Phi_{i,k}$
  for $k \in (1, 2, ..., K_2)$ **do**
    if $k < 10$ **then**
      $\Phi_{i,k+1} \leftarrow F(\phi_{i,k}, \Phi_{i,k}, n_3, r))$
    else
      $\Phi_{i,k+1} \leftarrow F(\phi_{i,k}, \Phi_{i,k}, n_4, r))$
  $\Phi^* = \Phi^* \cup \Phi_{i,K_2+1}$ ▷ $\phi^* \in \Phi^*$
  $\Phi^* \leftarrow F(\phi^*, \Phi^*, n_1, r)$

Table 1. Average method accuracy for simulation tests.

	Correct Landmark Pair % (100 Pairs)						
Transformation (U,V)	30%	40%	50%	60%	70%	80%	90%
U=0,V=0	NA	0.934	0.953	0.981	0.989	0.991	0.994
U=100, V=100	NA	0.923	0.948	0.978	0.984	0.985	0.991
U=sin(Y),V=cos(X)	NA	0.786	0.835	0.881	0.913	0.931	0.952
U=3sin(Y),V=3cos(X)	NA	0.403	0.623	0.781	0.842	0.876	0.921
U=7sin(Y),V=7cos(X)	NA	NA	NA	NA	0.697	0.742	0.838
	Correct Landmark Pair % (300 Pairs)						
Transformation (U,V)	30%	40%	50%	60%	70%	80%	90%
U=0,V=0	0.9222	0.945	0.979	0.984	0.991	0.993	0.995
U=100, V=100	NA	0.944	0.970	0.982	0.985	0.987	0.992
U=sin(Y),V=cos(X)	NA	0.878	0.892	0.914	0.938	0.947	0.965
U=3sin(Y),V=3cos(X)	NA	0.723	0.828	0.843	0.872	0.911	0.935
U=7sin(Y),V=7cos(X)	NA	NA	0.763	0.821	0.858	0.901	0.928
	Correct Landmark Pair % (700 Pairs)						
Transformation (U,V)	30%	40%	50%	60%	70%	80%	90%
U=0,V=0	0.946	0.969	0.978	0.990	0.993	0.995	0.998
U=100, V=100	0.934	0.950	0.976	0.985	0.991	0.993	0.995
U=sin(Y),V=cos(X)	NA	0.882	0.911	0.932	0.948	0.964	0.980
U=3sin(Y),V=3cos(X)	NA	0.779	0.846	0.872	0.915	0.931	0.949
U=7sin(Y),V=7cos(X)	NA	0.649	0.781	0.841	0.873	0.912	0.933

3. EXPERIMENT AND RESULTS

3.1. Validation with Simulated Landmark Pairs

To test the method efficacy, we randomly generate 100, 300, and 700 landmarks in a 3500×3500 image for the simulation test. In the simulation test, we set $K_1 = K_2 = 20$, $r = 1.1$, $n_1 = 2$, $n_2 = 3$, $n_3 = 1$, $n_4 = 4$. We copy all points from the reference image to a target image of the same size. These points have one-to-one mapping and serve as our initial landmark pairs. Next, we choose 10% to 80% of the total points on the target image, add random deformations subject to a normal distribution with zero mean and standard deviation 50 in both x and y directions. We consider deformed landmark pairs are outliers, and the remaining landmark pairs are correctly matched. Further, we apply multiple transformations to the reference image points to globally change landmark locations.

We apply our method to the simulated landmarks from the reference and target image space. The method accuracy is measured by the number of correct landmark pairs to the total number of correct pairs. For each pair of known transformation (U, V) and correct landmark pair percentage, we run 10 simulation tests and compute the average method accuracy.

Suggested by results in Table 1, our method improves the landmark pair accuracy by 42.6% on average. In general, a larger total pair number , a higher initial correct pair percentage, and a simpler transformation would lead to a higher accuracy. For example, given a non-transformed image, 90% of initial correct landmark pairs, and 700 total landmark pairs, the average accuracy reaches 99.8%.

However, one defect of our method is that it does not

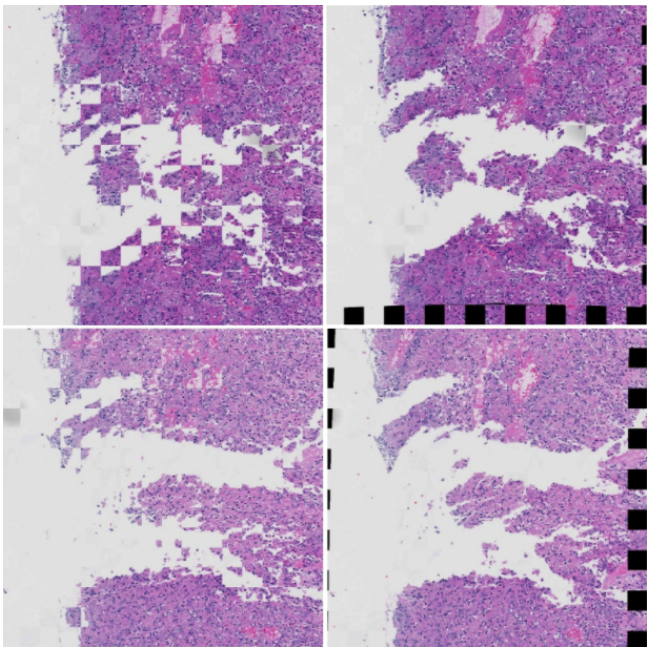

Fig. 2. Checkerboard view of adjacent histopathology images (Left) before and (Right) after our method application for two typical image regions.

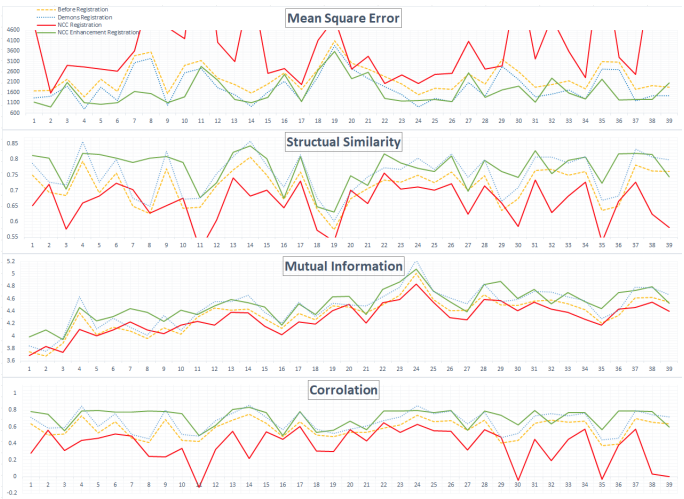

Fig. 3. correlation, structural similarity, mutual information and mean squared error comparison figure for not registered image(yellow), Demons image registration(blue), NCC selected landmark pair registered image(red) and trusted landmark pair registered image(green)

produce any output when the initial correct pair percentage is small (usually under 30%). This happens because our method cannot find the trusted landmark pair by their relative positions in the initial trusted pair identification stage. This results in absence of trusted pairs in the end.

3.2. Validation with Adjacent Histopathology Images

We further apply our method for trusted landmark pair selection and pruning with 40 Hematoxylin and Eosin-stained histopathology images of serial tissue sections that are approximately aligned by our prior method [12]. The initial landmark pairs are detected by the Normalized Cross-Correlation (NCC) method.

To evaluate the quality of our method, we compute Structural Similarity (SSIM), Mutual Information (MI), Correlation (COR), and Mean Squared Error (MSE) for each experiment. The registration quality before and after our method is compared. The comparison results suggest that our method improves the registration accuracy on average by 35.23% (COR), 17.56% (SSMI), 6.30% (MI), and 27.20% (MSE).

We present typical registration results in Figure **??**. On the left column, we present check-board views of two typical registered image regions with landmark pairs matched by NCC method. Apparently, the initial NCC landmark pairs does not work well for histopathology image registration. By contrast, we present, on the right column, the counterparts after registration with trusted landmark pairs from our method. The resulting registered images are well aligned with the corresponding reference images, suggesting the efficacy of our method for landmark pair selection.

4. CONCLUSION

We propose a method that automatically selects correct landmark pairs to improve the image registration performance. Our method produces initial trusted pairs by local landmark spatial patterns, and leverages them to generate more trusted pairs iteratively. The method is tested both on simulated landmark pairs and real serial histopathology images. Both quantitative and visual evaluation results suggest the promise of our proposed method for large-scale pathology image registration, which is the key to further development of 3D digital pathology analysis essential to tissue-based cancer research.

5. REFERENCES

[1] Aeffner, F., Zarella, M.D., et al., "Introduction to Digital Image Analysis in Whole-slide Imaging: A White Paper from the Digital Pathology Association," J Pathol Inform. 10(9), 2019

[2] Colling, R.Pitman, H. et al., "Artificial intelligence in digital pathology: a roadmap to routine use in clinical practice," J Pathol., 249(2):143-150, 2019.

[3] Kayser, K., Görtler, J. et al. "AI (artificial intelligence) in histopathology–from image analysis to automated diagnosis," Folia Histochem Cytobiol, 47(3):355-61, 2009.

[4] Clarke, E.L., Munnings, C., Williams, B., Brettle, D., Treanor, D.,"Display evaluation for primary diagnosis using digital pathology external site symbol," J. Med. Imag. 7(2), 2020.

[5] Williams, B.J., Ismail, A., Chakrabarty, A., Treanor, D., "Clinical digital neuropathology: experience and observations from a departmental digital pathology training programme, validation and deployment," Journal of Clinical Pathology 2020.

[6] Liang, Y. et al., "Liver whole slide image analysis for 3D vessel reconstruction," *Int. Symp. on Biomed. Imaging: From Nano to Macro*, pp. 1212–1215, 2015.

[7] Liang, Y. et al., "A framework for 3d vessel analysis using whole slide images of liver tissue sections," *Int. J. Comput. Biol. Drug Des.*, vol.9, pp. 102–119, 2016.

[8] Liang, Y.et al., "A 3d primary vessel reconstruction framework with serial microscopy images," *Int. Conf. on Med. Image Comput. Comput. Assist. Interv.*, pp. 251–259, 2015.

[9] Liang, Y.et al., "Development of a framework for large scale threedimensional pathology and biomarker imaging and spatial analytics," *In Proc. AMIA Jt. Summits on Transl. Sci.*, 2017.

[10] He, H., Razlighi Q., "Volumetric Registration of Brain Cortical Regions by Automatic Landmark Matching and Large Deformation Diffeomorphisms," *Proceedings of IEEE International Symposium on Biomedical Imaging*, vol.9993, pp. 1412-1417, 2020.

[11] Dalca, A.V., Bobu, A., Rost, N.S., Golland, P., "Patch-Based Discrete Registration of Clinical Brain Images," in *Patch Based Tech Med Imaging*, vol.9993, pp. 60-67, 2016.

[12] Rossetti, B.J., Wang, F.S., Zhang, P.Y., Teodoro, G., Brat, D.J., Kong, J., "Dynamic registration for gigapixel serial whole slide images," in *IEEE International Symposium on Biomedical Imaging*, pp. 424-428, 2017.

[13] Wang, S., Wang, T., Yang, L., Yang, D.M., Fujimoto, J., Yi, F., Luo, X., Yang, Y., Yao, B., Lin, S., Moran, C., Kalhor, N., Weissferdt, A., Minna, J., Xie, Y., Wistuba, I.I., Mao, Y., Xiao, G., "ConvPath: A Software Tool for Lung Adenocarcinoma Digital Pathological Image Analysis Aided by Convolutional Neural Network,"EBioMedicine, vol.50, pp. 385–395, 2017.